

# Flow-type landslides Impacting V-shaped Diversions: Physical Modelling

Ruoying Li<sup>1</sup>, and Clarence E. Choi<sup>1\*</sup>,

<sup>1</sup>The Department of Civil Engineering, The University of Hong Kong, HKSAR China

**Abstract.** In rural and sparsely populated areas, government issued pamphlets often recommend the construction of V-shaped diversions to protect personal property from flow-type landslides hazards, including debris flows. V-shaped diversions are advantageous because they attract low impact forces and runup heights due to their oblique impact angle. However, current design approaches are empirical, so it is unclear what resisting forces and wall heights are required. In this extended abstract, details of a new experimental setup and some preliminary results are presented. It is envisioned that findings from this study will help to shed light on scientific-based recommendations to design V-shaped diversions to enhance the resiliency of mountain communities globally.

## 1 Introduction

Flow-type landslides, including debris flows, snow avalanches, and granular flows, surge downslope under the influence of gravity and have been reported to cause fatalities and damage to infrastructure globally [1, 2, 3].

In rural areas, government-issued pamphlets recommend property owners to construct V-shaped diversions as personal protection against flow-type landslide hazards [3, 4]. Owing to an oblique impact orientation between a V-shaped diversion and a flow, the resisting force and runup heights are lower compared to an orthogonal impact orientation. This means that V-shaped diversions do not require designs that are bulky. Despite the high engineering value of V-shaped diversions, they are designed empirically. For example, Fig. 1. shows a conceptual schematic diagram of a V-shaped diversion [5]. It is recommended that the deflector angle should be “such that the area enclosed by the retaining walls is greater than the desired level area”, and “grade beam should extend two feet below the slope surface and be provided with three feet of freeboard”. Besides these recommendations, it is recommended that the design of diversions should follow the procedures for other retaining structures [5]. Evidently, conventional retaining structures and V-shaped diversions subjected to oblique dynamic loading are fundamentally different [6]. However, there is no guidance on the design wall height against runup and an optimised diversion angle to reduce the impact force [7, 8].

In this study, a new experimental setup, along with its instrumentation and modelling procedures is presented. Then, some preliminary results are shown. It is expected that the findings from this study will help to progress towards scientific-based design guidance for V-shaped diversions to empower vulnerable

communities in mountainous regions to protect themselves from debris flow hazards.

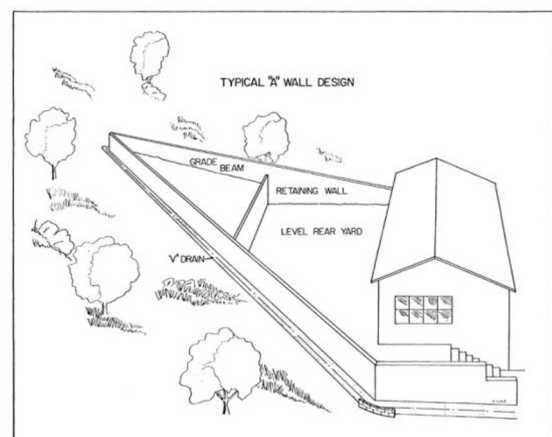


Fig. 1. Schematic diagram of a typical V-shaped diversion [5].

## 2 Methodology

Figure 2 shows the new experimental model developed for this study. It consists of a flume, which has a length of 1.5 m, a width of 0.2 m, and a depth of 0.3 m. The flume consists of a 0.3 m long container for storing the geomaterial initially at the upstream end. The inclination of the flume is selected to be  $\zeta = 35^\circ$  to generate high energy flows on obstacles [9, 10].

The diversions are designed with three different diversion angles  $\alpha$  (i.e.,  $30^\circ$ ,  $60^\circ$ ,  $120^\circ$ ) while keeping the distance  $d$  between the two side walls constant. A Froude number  $Fr$  of 6 is selected to model supercritical flow [11, 12].

\* Corresponding author: [cechoi@hku.hk](mailto:cechoi@hku.hk)

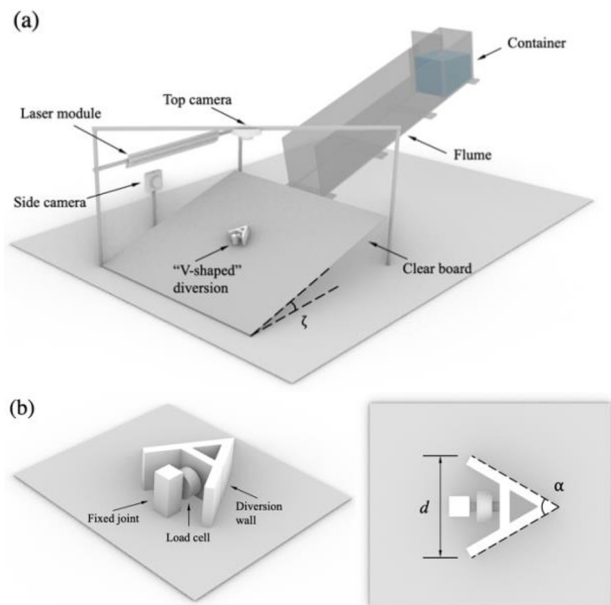


**Fig. 2.** A new experimental model (a) Oblique schematic with a slope angle  $\zeta$  for both the flume and the clear board; (b) Diversion details.

### 2.1 Instrumentation

Top- and side-view cameras (i.e., 240 frames per second at a resolution of  $1920 \times 1080$ ) are mounted around the model to capture the flow and impact behaviour. A load cell is sandwiched between a fixed joint and a frontal diversion wall. Laser cartography is adopted to measure the spatiotemporal changes in flow height. This method makes use of refracted laser beams and the shadow bar technique to capture dynamic changes in the flow height. The laser beams pass through vertically placed cylindrical lens and are then refracted to a surface [13]. The height difference is proportional to the difference between the original reference line and the distorted line, which needs to be calibrated using a standard object with a known height beforehand. The contour of the thickness can then be deduced from the captured images [14]. This method has been successfully evaluated by McDonald and Anderson in 1996 [15].

### 2.2 Modelling procedures

In each model test, the model diversion is installed on an unchannelised board with dimensions of 1.0 m by 1.0 m to enable the impact behaviour to be studied. The diversion is affixed orthogonally to an inclined clear board with a fixed joint behind the V-shaped walls. High-speed cameras are then mounted around the model. Geomaterial is prepared in the storage container at the upstream end of the flume. The material is retained by a gate, which is released by lifting it vertically. The granular material used in the test is the Toyoura sand. A total mass of 10 kg is prepared, and then the flume is inclined to the target angle. Afterwards, the granular material is released from the container. The flow accelerates down the flume under the influence of gravity and impacts the model diversion.

## 3 Preliminary results

Figure 3 shows the impact behaviour as captured by the top camera. Grids on the board are spaced at an interval of 100 mm. The apex of the model diversion is placed 200 mm downstream from the mouth of the flume. The flow impacts the diversion (i.e.,  $\alpha = 30^\circ$ , and  $d = 100$  mm).

It can be observed that oblique shocks form when the granular flow impacts the diversion. The shock angle  $\beta$  at quasi-steady state is approximately  $80^\circ$ . At the apex of the diversion wall, the granular material is observed to jump and form a stagnation point. The observed impact can be used to evaluate analytical formulations for predicting the runup height and impact force.

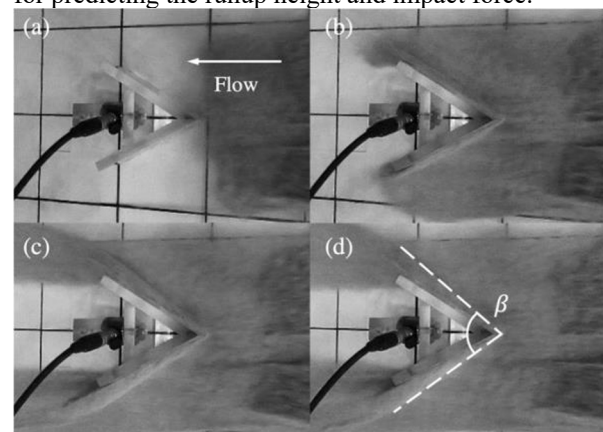


**Fig. 3.** Oblique shock evolution with time from (a) initial impact to (d) steady state flow.

## 4 Summary

Diversion structures are more compact alternatives compared to traditional rigid barriers because they deflect the flow material to reduce the impact force and runup height. The described experimental model setup in this extended abstract will be used to optimise the the diversion angle, impact force, and wall height for a wide range of flow types. It is envisioned that findings from this study can be used to rationalise the design of V-shaped diversions for vulnerable communities globally.

The work described in this extended abstract is supported by the HKU Presidential PhD Scholar Programme (HKU-PS). The authors are grateful for the financial sponsorship from The University of Hong Kong.

### References

- O. Hungr, S. G. Evans, M. J. Bovis, and J. N. Hutchinson, *Environ. Eng. Geosci.*, vol. 7, no. 3, pp. 221–238, doi: 10.2113/gsegeosci.7.3.221 (2021)
- J. S. H. Kwan *et al.*, *Trans. Hong Kong Inst. Eng.*, vol. 25, no. 2, pp. 90–101, doi: 10.1080/1023697X.2018.1462105 (2018)
- Colorado Geological Survey (CGS), no. HAZ-2021-01, Available: <https://coloradogeologicalsurvey.org/publications/post-wild/re-mud-slides-debris-%22ows> (2021)

4. California Geological Survey (CGS), CGS Note 33 (2003)
5. R. Hollingsworth and G. S. Kovacs, *Environ. Eng. Geosci*, vol. **18**, no. 1., pp. 17–28, doi: [10.2113/gsegeosci.xviii.1.17](https://doi.org/10.2113/gsegeosci.xviii.1.17) (1981)
6. P. Song and C. E. Choi, *J Geophys Res Earth Surf*, vol. **126**, no. 5, doi: [10.1029/2020JF005930](https://doi.org/10.1029/2020JF005930) (2021)
7. T. Jóhannesson, M. Barbolini, P. Gauer, and U. Domaas, pp. 212 (2009)
8. A. B. Prochaska, P. M. Santi, and J. D. Higgins, *Environ. Eng. Geosci*, vol. **14**, no. 4, pp. 297–313, doi: [10.2113/gsegeosci.14.4.297](https://doi.org/10.2113/gsegeosci.14.4.297) (2008)
9. K. M. Hákonardóttir and A. J. Hogg, *Phys. Fluids*, vol. **17**, no. 7, pp. 1–10, doi: [10.1063/1.1950688](https://doi.org/10.1063/1.1950688) (2005)
10. X. Cui and J. M. N. T. Gray, *J Fluid Mech*, vol. **720**, pp. 314–337, doi: [10.1017/jfm.2013.42](https://doi.org/10.1017/jfm.2013.42) (2013)
11. R. M. Iverson, D. L. George, and M. Logan, *J Geophys Res Earth Surf*, vol. **121**, no. 12, pp. 2333–2357, doi: [10.1002/2016JF003933](https://doi.org/10.1002/2016JF003933) (2016)
12. C. Tregaskis, C. G. Johnson, X. Cui, and J. M. N. T. Gray, *J Fluid Mech*, vol. **933**, doi: [10.1017/jfm.2021.1074](https://doi.org/10.1017/jfm.2021.1074) (2022)
13. R. M. Iverson, M. Logan, and R. P. Denlinger, *J Geophys Res Earth Surf*, vol. **109**, no. F1, doi: [10.1029/2003jf000084](https://doi.org/10.1029/2003jf000084) (2004)
14. O. Pouliquen and Y. Forterre, *J Fluid Mech*, vol. **453**, pp. 133–151, doi: [10.1017/S0022112001006796](https://doi.org/10.1017/S0022112001006796) (2002)
15. R. R. McDonald and R. S. Anderson, *J. Sediment. Res.*, vol. **66**, no. 3, pp. 642–653, doi: [10.1306/D42683D3-2B26-11D7-8648000102C1865D](https://doi.org/10.1306/D42683D3-2B26-11D7-8648000102C1865D) (1996)